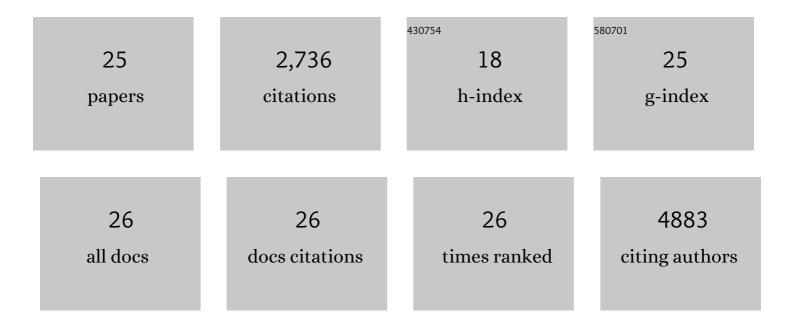
## Rachael L Terry

List of Publications by Year in descending order

Source: https://exaly.com/author-pdf/5392036/publications.pdf Version: 2024-02-01



#	Article	IF	CITATIONS
1	Osteoclasts recycle via osteomorphs during RANKL-stimulated bone resorption. Cell, 2021, 184, 1330-1347.e13.	13.5	203
2	Dual Targeting of Chromatin Stability By The Curaxin CBL0137 and Histone Deacetylase Inhibitor Panobinostat Shows Significant Preclinical Efficacy in Neuroblastoma. Clinical Cancer Research, 2021, 27, 4338-4352.	3.2	14
3	Chimeric Antigen Receptor T cell Therapy and the Immunosuppressive Tumor Microenvironment in Pediatric Sarcoma. Cancers, 2021, 13, 4704.	1.7	9
4	Enhancing the Potential of Immunotherapy in Paediatric Sarcomas: Breaking the Immunosuppressive Barrier with Receptor Tyrosine Kinase Inhibitors. Biomedicines, 2021, 9, 1798.	1.4	6
5	Immune profiling of pediatric solid tumors. Journal of Clinical Investigation, 2020, 130, 3391-3402.	3.9	27
6	A niche-dependent myeloid transcriptome signature defines dormant myeloma cells. Blood, 2019, 134, 30-43.	0.6	99
7	Melphalan modifies the bone microenvironment by enhancing osteoclast formation. Oncotarget, 2017, 8, 68047-68058.	0.8	10
8	Osteoclasts control reactivation of dormant myeloma cells by remodelling the endosteal niche. Nature Communications, 2015, 6, 8983.	5.8	296
9	Defective Inflammatory Monocyte Development in IRF8-Deficient Mice Abrogates Migration to the West Nile Virus-Infected Brain. Journal of Innate Immunity, 2015, 7, 102-112.	1.8	20
10	Anti-Sclerostin Treatment Prevents Multiple Myeloma Induced Bone Loss and Reduces Tumor Burden. Blood, 2015, 126, 119-119.	0.6	14
11	The Bacteriostatic Protein Lipocalin 2 Is Induced in the Central Nervous System of Mice with West Nile Virus Encephalitis. Journal of Virology, 2014, 88, 679-689.	1.5	21
12	Molecular control of monocyte development. Cellular Immunology, 2014, 291, 16-21.	1.4	56
13	Therapeutic Inflammatory Monocyte Modulation Using Immune-Modifying Microparticles. Science Translational Medicine, 2014, 6, 219ra7.	5.8	284
14	Experimental Autoimmune Encephalomyelitis in Mice. Methods in Molecular Biology, 2014, 1304, 145-160.	0.4	58
15	Virus infection, antiviral immunity, and autoimmunity. Immunological Reviews, 2013, 255, 197-209.	2.8	238
16	Enhanced Efferocytosis of Apoptotic Cardiomyocytes Through Myeloid-Epithelial-Reproductive Tyrosine Kinase Links Acute Inflammation Resolution to Cardiac Repair After Infarction. Circulation Research, 2013, 113, 1004-1012.	2.0	268
17	Antiviral macrophage responses in flavivirus encephalitis. Indian Journal of Medical Research, 2013, 138, 632-47.	0.4	9

18 Current Theories for Multiple Sclerosis Pathogenesis and Treatment. , 2012, , .

0

RACHAEL L TERRY

#	Article	IF	CITATIONS
19	Microparticles bearing encephalitogenic peptides induce T-cell tolerance and ameliorate experimental autoimmune encephalomyelitis. Nature Biotechnology, 2012, 30, 1217-1224.	9.4	351
20	Mice Deficient in STAT1 but Not STAT2 or IRF9 Develop a Lethal CD4 <sup>+</sup> T-Cell-Mediated Disease following Infection with Lymphocytic Choriomeningitis Virus. Journal of Virology, 2012, 86, 6932-6946.	1.5	44
21	Targeted blockade in lethal West Nile virus encephalitis indicates a crucial role for very late antigen (VLA)-4-dependent recruitment of nitric oxide-producing macrophages. Journal of Neuroinflammation, 2012, 9, 246.	3.1	65
22	Inflammatory monocytes and the pathogenesis of viral encephalitis. Journal of Neuroinflammation, 2012, 9, 270.	3.1	105
23	IFN Regulatory Factor 8 Is a Key Constitutive Determinant of the Morphological and Molecular Properties of Microglia in the CNS. PLoS ONE, 2012, 7, e49851.	1.1	66
24	Tolerance Induced by Apoptotic Antigen-Coupled Leukocytes Is Induced by PD-L1+ and IL-10–Producing Splenic Macrophages and Maintained by T Regulatory Cells. Journal of Immunology, 2011, 187, 2405-2417.	0.4	182
25	Ly6c+ "inflammatory monocytes―are microglial precursors recruited in a pathogenic manner in West Nile virus encephalitis. Journal of Experimental Medicine, 2008, 205, 2319-2337.	4.2	289